Available online at BCREC website: https://bcrec.id

Bulletin of Chemical Reaction Engineering & Catalysis, 18 (1) 2023, 37-47

Research Article

Selective Adsorption of Direct Group Anionic Dyes on Layered Double Hydroxide-Chitosan Composites

Neza Rahayu Palapa[1,2], Nova Yuliasari[3], Patimah Mega Syah Bahar Nur Siregar[2], Alfan Wijaya[2], A. Amri[2], Nur Ahmad[3], Aldes Lesbani[2,3,*]

[1]Department of Chemistry, Faculty of Mathematics and Natural Sciences, Sriwijaya University, Palembang, 30662, Indonesia
[2]Research Center of Inorganic Materials and Complexes, Faculty of Mathematics and Natural Sciences, Sriwijaya University, Palembang, 30139, Indonesia
[3]Graduate School of Mathematics and Natural Sciences, Faculty of Mathematics and Natural Sciences, Sriwijaya University, Palembang, 30139, Indonesia.

Received: 20th December 2022; Revised: 26th January 2023; Accepted: 26th January 2023
Available online: 27th January 2023; Published regularly: March 2023

Abstract

In this research, the potential of M^{2+}/Al intercalated chitosan has been evaluated and good ability to reduce dyes in an aqueous solution. M^{2+}/Al intercalated chitosan was prepared by anion exchange method and coprecipitation in a nitrogen atmosphere. Selectivity adsorption was studied to maintain the ability of M^{2+}/Al intercalated chitosan for particle size of direct dyes (direct green, direct red, and direct yellow). To evaluate the adsorption process, M^{2+}/Al intercalated chitosan was conducted with kinetic, isotherm, and thermodynamic parameters. The kinetic data fitted well by pseudo-second order and isotherm fitted Langmuir isotherm with q_{max} obtained 294.11 and 322.58 mg/g for Zn/Al-chitosan and Mg/Al-chitosan, respectively.

Keywords: Selectivity Dye Adsorption; Intercalated; Chitosan; Mg/Al LDH; Zn/Al LDH

How to Cite: N.R. Palapa, N. Yuliasari, P.M.S.B.N. Siregar, A. Wijaya, A. Amri, N. Ahmad, A. Lesbani (2023). Selective Adsorption of Direct Group Anionic Dyes on Layered Double Hydroxide-Chitosan Composites. *Bulletin of Chemical Reaction Engineering & Catalysis*, 18(1), 37-47. (doi: 10.9767/bcrec.16795)

Permalink/DOI: https://doi.org/10.9767/bcrec.16795

1. Introduction

Adsorption efficiently removes wastewater pollutants, such as metal ions, organic contaminants, and hazardous materials [1,2]. This method has been used for a long time due to its simple way, easy process, and no side effect [3]. This method's efficiency depends on the quality of the adsorbents to remove wastewater. Various adsorbents have been tested and reported by many researchers to remove pollutants from wastewater from inorganic to organic materials such as zeolite [4], bentonite [5], kaolinite [6], layered double hydroxide [7], chitin [8], cellulose [9], chitosan [10], lignite [11], and also various hybrid materials including composites [12].

Layered double hydroxides have been widely used as potential adsorbents for pollutants ranging from inorganic to organic waste [13]. The chemical formula of layered double hydroxide consists of divalent and trivalent metals ion on periodic elements and these compounds are generally written as M^{2+}/M^{3+} materials. The common chemical structure of layer double hydroxide is $[M^{2+}_{1-x}M^{3+}_{x}(OH)_2]^{x+}[(A^{m-})_{x/m}.nH_2O]^{x}$, where M^{2+} and M^{3+} are divalent and trivalent ions, and A^{m-} is charge bal-

* Corresponding Author.
Email: aldeslesbani@pps.unsri.ac.id (A. Lesbani)

ancing interlayer anion [14–16]. Layered double hydroxide can also modify the interlayer of the surface of the material by large anion or high structural compact materials such as carbon-based materials. Modification of layered double hydroxide on interlayer has been conducted by Palapa *et al.* [17] also use polyoxometalate as intercalant to increase interlayer space for Ni/Al LDH adsorption of malachite green. On the other hand, modification of layered double hydroxide by carbon materials such as biochar [18], hydrochar [19], and graphite [20] has been conducted to increase the adsorption capacity of layered double hydroxide as an adsorbent.

Development and the use of various synthetic dyes in textile, photography, arts, painting, and pharmaceuticals are sharply increasing; thus, the treatment of wastewater dyes is important [21]. The composition of dyes cannot be determined directly in nature wastewater due to the mixing of pollutants [22]. In this case, adsorption is a relatively unuseful method to reduce dyes from wastewater [23]. The selectivity process is critical to eliminate dye pollutants by the selective adsorbent.

Many researchers conducted several reports to apply layered double hydroxide for water pollution remediation. Yadav and Dasgupta [2] prepared an aqueous solution of Mg/Al LDH intercalated nitrate anion for methyl orange dye. Kameda *et al.* [24] reported lactate adsorption using Cu/Al LDH. Missau *et al.* [25] Ca/Al supported by biochar was conducted to remove crystal violet in an aqueous solution. Among all this literature, the researchers had a good performance in the remediation of water pollution after modifying layered double hydroxide, not at pristine condition.

Modifying layered double hydroxide by biochar and hydrochar can create high surface area properties and adsorption capacity [26], but these materials are unselective for several dyes [27]. Chitosan is natural carbon-based material with high availability from crustacean shells. Chitosan can also be used as carbon-based material to layered double hydroxide to form double hydroxide/chitosan composites. Using chitosan can increase surface area, adsorption capacity, and high selectivity of adsorbed dye in an aqueous solution [28]. So, in this research, layered double hydroxide M^{2+}/Al was prepared by an intercalating process with chitosan to obtain the selective adsorbent with good adsorption performance. The adsorption study was conducted to adsorb direct dyes selective in aqueous solutions such as direct red, direct green, and direct yellow-12. The adsorption study, such as kinetic, isotherm, thermodynamic study, and adsorption mechanism, was also evaluated in this research.

2. Materials and Methods

2.1 Chemicals and Instrumentation

Chemicals were supplied from Sigma Aldrich and Merch, such as zinc nitrate, aluminum nitrate, magnesium nitrate, and sodium hydroxide. Deionized water was supplied from the Research Centre of Inorganic Materials and Complexes. Water was deionized by Purite® ion exchange resin by several cycles. Analysis of adsorbent was performed by Rigaku- Miniflex-600 X-Ray Diffraction (XRD). Scanning of the sample was conducted at 1°/min. Analysis of Fourier Transform Infra Red (FTIR) was performed by Shimadzu Prestige-21 FTIR spectrophotometer and the sample was mixed with KBr to form a pellet. The sample was scanned at wavenumber 500-4000 cm^{-1}. Brunauer-Emmett-Teller (BET) surface area analysis was conducted using Quantachrome Micrometric 2020, and the sample was degassed under liquid N_2 prior to analysis. Scanning Electron Microscope-Energy Dispersive X-ray (SEM-EDX) Type Quanta-650 Oxford. Anionic dyes were analyzed by UV-Visible spectrophotometer Bio-Base BK-UV 1800 PC.

2.2 Preparation of Layered Double Hydroxide Zn/Al and Mg/Al

Synthesis of layered double hydroxide Zn/Al and Mg/Al was carried out using zinc nitrate, aluminum nitrate, and magnesium nitrate. Zinc nitrate (0.75 M, 100 mL) was mixed with aluminum nitrate (0.25 M, 100 mL) on a Beaker glass equipped with a magnetic bar and hot plate. Sodium hydroxide (2 M) was added slowly to the reaction mixture and pH was adjusted to 10. The reaction mixture was kept at 80 °C for 20 h. Then white powder of Zn/Al layered double hydroxide was washed with water several times and dried at 120 °C. The synthesis of Mg/Al layered double hydroxide was carried out similarly with Zn/Al with a molar ratio of M^{2+}/M^{3+} was 3:1. Materials were characterized by XRD powder, FTIR, BET and SEM-EDX analyses.

2.3 Preparation of Zn/Al-Chitosan and Mg/Al-Chitosan

Composites of Zn/Al-Chitosan and Mg/Al-Chitosan were prepared by mixing layered double hydroxide and chitosan through the co-

precipitation method with slightly modified from [29]. The solution of M^{2+}/M^{3+} (M^{2+} = Zn, Mg; M^{3+} = Al) with molar ratio 3:1 was mixed and pH was adjusted to 10 by adding 2 M sodium hydroxide. The reaction was stirred for 1 h and 3 g of chitosan was added. The reaction was performed for 72 h at 80 °C. Composite was obtained and dried at 120 °C overnight. Materials were characterized by XRD, FTIR, BET Surface area, and SEM-EDX analyses.

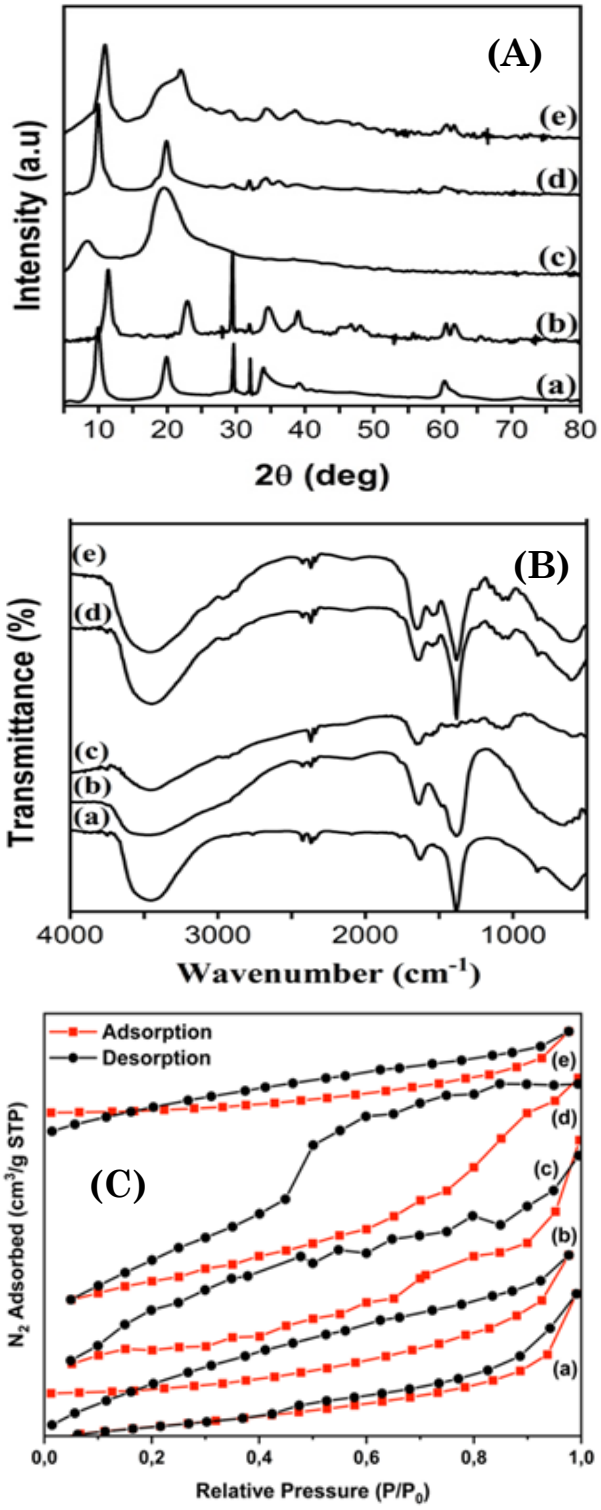

Figure 1. XRD powder pattern (A), FTIR spectrum (B) and pattern of adsorption-desorption of nitrogen (C); Zn/Al (a), Mg/Al (b), Chitosan (c), Zn/Al-Chitosan (d), and Mg/Al-Chitosan (e).

2.4 Adsorption Study and Mechanism

The selectivity adsorption of dyes on Zn/Al, Mg/Al, Zn/Al-Chitosan, and Mg/Al-Chitosan was carried out using direct green (λ = 622 nm), direct red (λ = 495 nm), and direct yellow-12 (λ = 414 nm) as anionic dyes. All anionic dyes with equal volume were mixed with each adsorbent and the concentration of dyes was monitored several times using UV-visible spectrophotometer analysis. The fast-decreasing absorbance for each anionic dye was analyzed and selective dyes were obtained for each adsorbent. Adsorption was conducted by a batch method using selective dye on layered double hydroxides and composites. Adsorption was studied by the effect of adsorption time, initial concentration of anionic dye and adsorption temperature. The effect of adsorption time was conducted in the range of 10-1500 min. The effect of the initial concentration of selective dye was conducted in the range of 10-120 mg/L for temperatures 30-60 °C. Analysis of the dye was performed using UV-Visible spectrophotometer.

3. Results and Discussion

The XRD pattern is shown in Figure 1(A). The Mg/Al and Zn/Al LDH diffractograms show peaks at 10°, 28°, 35°, and 60° that correspond to reflection planes 003, 006, 012, and 110, respectively, which indicates that the material has a layered structure (JCPDS 38-0478; 38-0486). The broad peak visible at 24° (as shown in Figure 1(A) (a; d and e) corresponds to reflection plane 002 on the surface of the LDH due to the presence of chitosan following the intercalation with LDH [30]. Furthermore, the interlayer space of the Mg/Al and Zn/Al LDH was increased after the intercalation. This increase in the interlayer space was related to

Table 1. Adsorbents properties.

Materials	S_{area} (m^2/g)	Interlayer Space (Å)
Mg/Al	5.84	7.67
Zn/Al	2.88	6.29
Chitosan	8.55	-
Mg/Al-Chitosan	24.55	9.84
Zn/Al-Chitosan	8.96	6.31

the increased surface area. The findings of the surface area analysis revealed that the intercalation process was successful (Table 1).

The FTIR spectra of the Mg/Al, Zn/Al, chitosan, and its intercalation are shown in Figure 1(B). The broad vibration of the hydroxyl groups (O−H stretching) in the brucite layers and interlayer space was confirmed at 3400–3600 cm^{-1} for all the materials. The lower vibration seen at 1635 cm^{-1} stems from the O−H bending. The nitrate anion from the interlayer Mg/Al, Zn/Al LDH, and its modification was confirmed by the intense peak visible at 1381 cm^{-1}. The chitosan's spectrum shows a low-intensity peak at 1033 cm^{-1}, which denotes the stretching vibration of the C−O. The adsorption-desorption pattern of nitrogen by the BET method was shown in Figure 1(C). Figure 1(C) showed that these materials dominant have a loop hysteresis curve and indicate that the material has irregular pores and shapes. Thus, the properties material such as surface area, has been mentioned in Table 1.

Figure 2 shows the scanning electron microscope (SEM) of materials. The SEM analyses are used as morphological of observed objects. As shown in Figure 2, the composite material is slightly different from LDH pristine. The pristine LDH (c and d) showed the hexagonal morphology with sharp edges and a smooth surface which indicate the formation of well-ordered LDH. The SEM images of composite materials (a and b) showed the particles are agglomerated, the surfaces are more diffused,

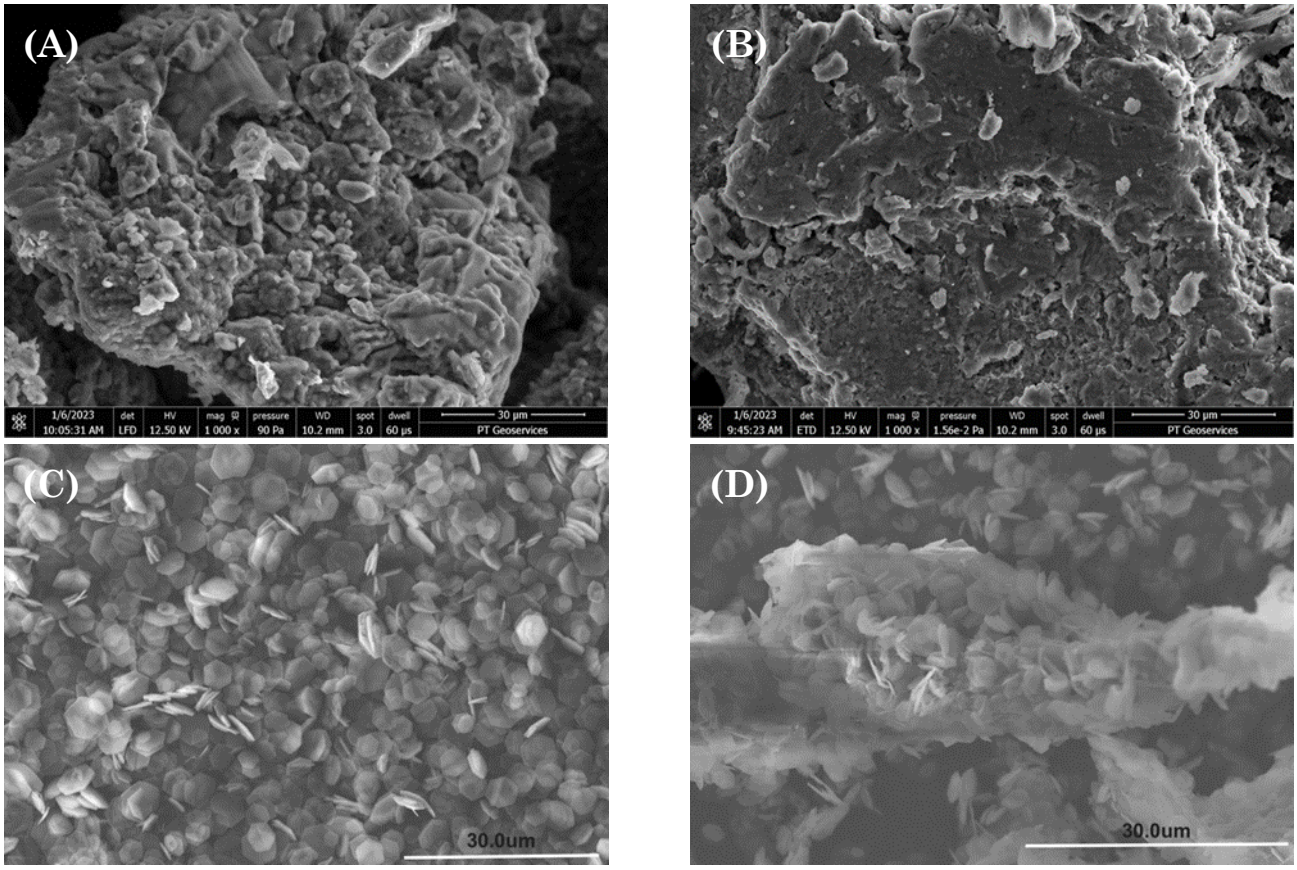

Figure 2. SEM of Mg/Al-Chitosan (a), Zn/Al-Chitosan (b), Mg/Al (c), dan Zn/Al (d).

Table 2. EDS Analysis of Zn/Al-Chitosan and Mg/Al-Chitosan.

Materials	Zn/Al-Chitosan	Zn/Al	Mg/Al-Chitosan	Mg/Al
C	7.52	-	7.97	-
N	4.39	-	14.67	-
O	38.33	40.7	52.23	32.35
Na	5.66	2.0	16.58	-
Al	5.77	9.9	4.71	16.63
Zn	38.33	47.4	-	-
Mg	-	-	3.85	51.02
Total	100	100	100	100

and the edges are not as sharp as that of LDH pristine, suggesting that there might be excess SDS draped over the particles on the outer surfaces. The particles were found to be more irregular in size due to the incorporation of the organic molecules. The EDX also showed the EDX results (Table 2) indicated the presence of C atoms after the LDH-chitosan composite process. However, for pure LDH there is no C atom in the LDH composition. This assumed that the formation of composite materials was successful.

To determine the adsorption capacities, all the adsorbents were tested in terms of their capacity to remove the dye mixture. It should be noted that the selective adsorption of the mixture is considered the most important and challenging when it comes to competitive dye adsorption. Therefore, mixtures of three direct types of dye solutions (*i.e.*, DY, DG, and DR) were also investigated in the adsorption experiments concerning all the adsorbents, as shown in Figure 3.

The DY solution showed the most effective and preferential adsorption in the mixing solutions using Mg/Al-chitosan and Zn/Al-chitosan after 180 min, while the DR solution showed slightly decreased adsorption after 180 min and the DG solution showed hardly any adsorption. This phenomenon indicated that the larger surface area of the Mg/Al-chitosan and Zn/Al-chitosan when compared with the pristine LDH affected the adsorption of the

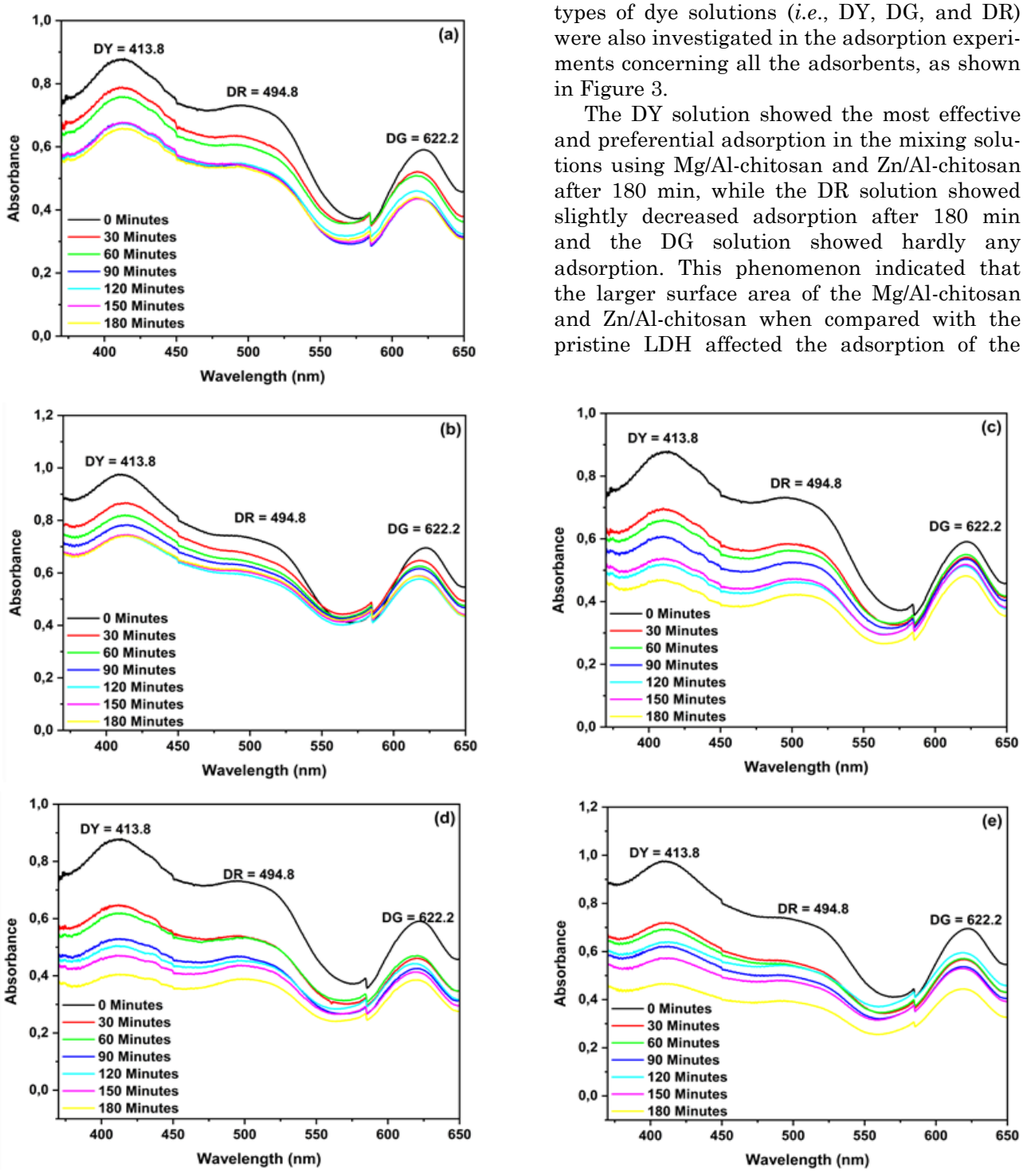

Figure 3. UV-Vis spectrum of various cationic dyes in the adsorption on Zn/Al (A), Mg/Al (B), Chitosan (C), Zn/Al-Chitosan (D), and Mg/Al-Chitosan (E).

cationic DY. In addition, the moderate adsorption ability of the DR and DG solutions when compared with the DY solution was likely caused by DY solution having four more probabilities of interaction with the interlayer space or surface of the adsorbents. Thus, the Mg/Al-chitosan showed good adsorption ability and selectivity toward the direct dye solutions.

Based on the selectivity results, the DY solution can be more easily adsorbed than the DR and DG solutions. More specifically, the DY solution was selected as a representative dye to determine the adsorption capacity in a watery solution. The effect of the adsorption time was tested to all the adsorbents. Figure 4 shows the time taken to adsorb the DY solution by all the adsorbents. According to these findings, a higher adsorption capacity was exhibited by the LDH-chitosan than the pristine varieties, with the dye adsorbed being 37 mg/L and 36 mg/L for the Mg/Al-chitosan and Zn/Al-chitosan, respectively. Moreover, the adsorption capacity was calculated using the pseudo-first-order (PFO) (Equation (1)) and pseudo-second-order (PSO) (Equation (2)) reactions, as similarly reported by [2].

$$\log\left(q_e - q_t\right) = \log q_e - \frac{k_1 t}{2.303} \quad (1)$$

$$\frac{t}{q_t} = \frac{1}{k_2 q_e^2} + \frac{1}{q_e} t \quad (2)$$

where, q_e denotes the adsorption capacity at equilibrium, k_1 is the rate constant of the PFO reaction, and k_2 is the rate constant for the PSO reaction. The rate constant was obtained by plotting each equation to determine the correlation coefficients (Table 3).

The parameters and correlation coefficients (R^2) obtained from the linear plotting log (q_e–q_t) vs. t (PFO reaction) and t/q_t vs. t (PSO reaction) are listed in Table 3.

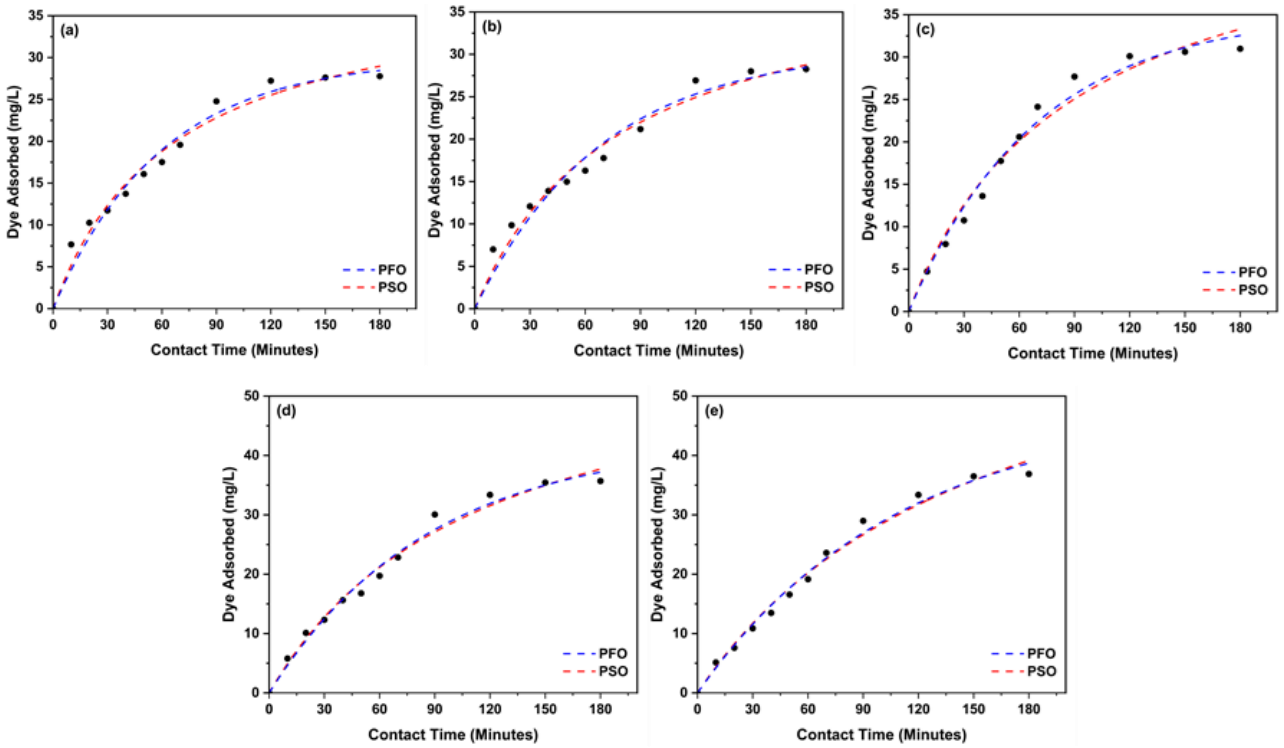

Figure 4. Effect of adsorption time and kinetic profile of DY on Zn/Al (a), Mg/Al (b), Chitosan (c), Zn/Al-Chitosan (d), and Mg/Al-Chitosan (e).

Table 3. Kinetic parameter of DY.

Adsorbent	$q_{e(exp)}$ (mg/g)	PFO			PSO		
		$q_{e(calc)}$ (mg/g)	R^2	k_1	$q_{e(calc)}$ (mg/g)	R^2	k_2
Zn/Al	27.774	44.968	0.925	0.034	37.736	0.963	0.0005
Mg/Al	28.262	41.957	0.881	0.028	38.911	0.951	0.0004
Chitosan	30.979	47.381	0.961	0.031	50.761	0.912	0.0002
Zn/Al-Chitosan	35.697	58.857	0.892	0.030	58.824	0.947	0.0002
Mg/Al-Chitosan	36.877	59.662	0.882	0.027	74.074	0,911	0.0001

In all cases, the results show that based on the R^2, the pseudo-second-order reaction is preferred over the pseudo-first-order reaction. This finding is supported by the $q_{e(calc)}$ PSO, which is close to the $q_{e(exp)}$. This indicates that the adsorption follows the pseudo-second-order kinetic model, which suggests the influence of the electrostatic attraction stemming from the adsorbate-adsorbent mixture. In addition, the increasing k_2 values after the composites are reflected in the shorter time required by the respective systems to achieve equilibrium. In other words, a higher k_2 value indicates that the adsorbate molecule is in a reactive condition [31].

The effects of the temperature and initial DY concentration on the dye uptake of all the adsorbents were also evaluated. The effect of the temperature was investigated over the temperature range 303–333 K. Figure 5 (a–c) presents the DY uptake in several concentrations for the pristine LDH and chitosan. Higher DY removal was observed at 333 K. Figure 5 (d–e) shows the higher DY uptake at 333 K too, although higher DY adsorbent capacity was obtained by the Mg/Al-chitosan. The increasing dye uptake with the increasing temperature caused a decrease in the solution's viscosity and an increase in its porosity or interlayer space, thereby resulting in the enhancement of the active sites for the adsorbent [32].

These results were calculated using the Freundlich and Langmuir adsorption isotherms. The linear forms of the Langmuir (Equation (3)) and Freundlich (Equation (4)) isotherms are as follows:

$$\frac{C_e}{q_e} = \frac{1}{q_{\max}} C_e + \frac{1}{q_{\max} k_L} \tag{3}$$

$$\ln q_e = \ln k_F + \frac{1}{n} \ln C_e \tag{4}$$

where, $q_{\max}$ and k_L are the Langmuir constants, k_F and n are the Freundlich constants, and n indicates a favorable adsorption process and verifies the type of adsorption that occurs. The isotherm adsorption parameters are shown in Table 4.

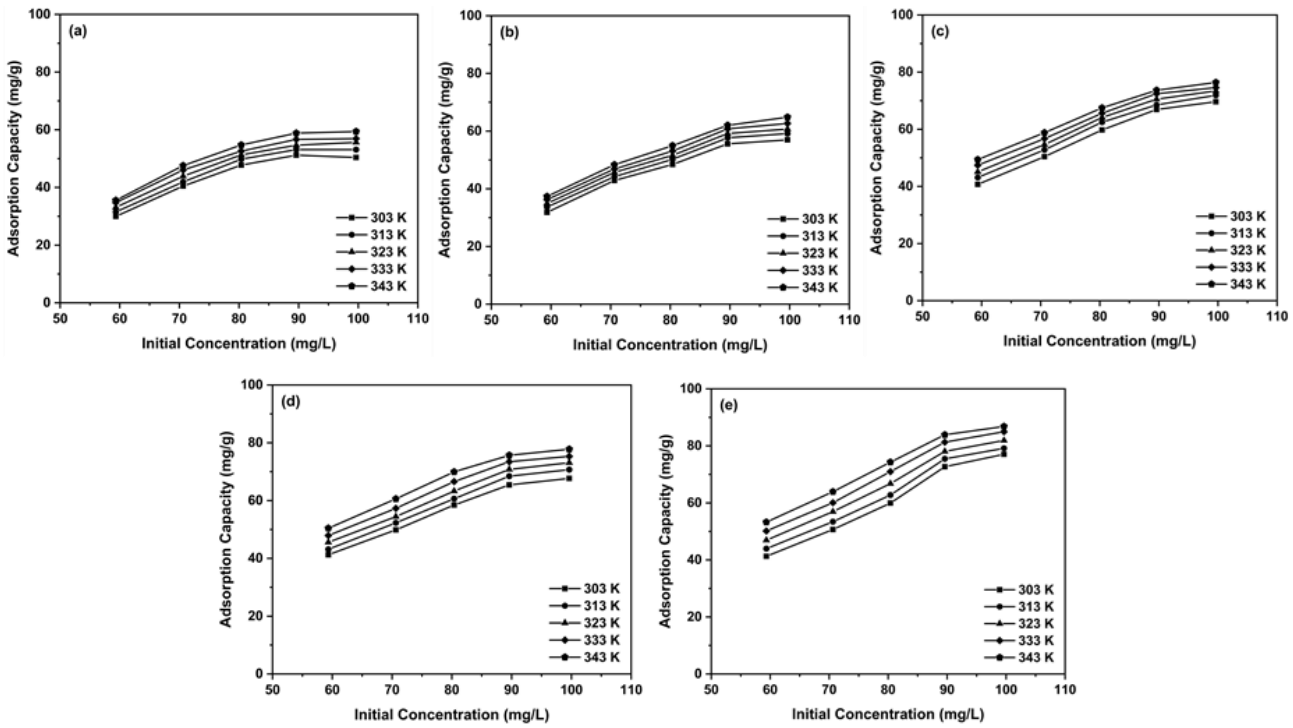

Figure 5. Isotherm adsorption of DY on Zn/Al (a), Mg/Al (b), Chitosan (c), Zn/Al-Chitosan (d), and Mg/Al-Chitosan (e).

Table 4. Isotherm adsorption of DY.

Adsorption Constants	Zn/Al	Mg/Al	Chitosan	Zn/Al-Chitosan	Mg/Al-Chitosan
q_{max}	68.02	135.13	119.04	294.11	322.58
k_L	0.025	0.022	0.085	0.01	0.01
n	1.354	1.012	2.063	1.181	1.487
k_F	3.105	1.77	17.828	3.921	7.984

In all cases, the results indicated that the R^2 was better for the Langmuir isotherm than the Freundlich isotherm, suggesting that the adsorption of DY by the adsorbents involved monolayer adsorption. All the materials showed spectacular adsorption and an increasing q_{max} almost four times that of the pristine varieties. The highest adsorption capacity was obtained by the Mg/Al-chitosan and Zn/Al-chitosan (322.58 mg/g and 294.11 mg/g, respectively). These findings indicate that the modification of LDH using chitosan resulted in more effective adsorption than the other modifications of the adsorbents shown in Table 5.

The mechanism of adsorption, the rate-limiting step, and the dependent factors can be utilized to understand the complex mechanism of adsorption [27]. According to Li *et al.* [38] the adsorption onto active adsorbent sites can occur through chemical and physical adsorption. The notes of physisorption can be displaced as the rapid occurrence of kinetics adsorption. Furthermore, based on the results in kinetics data, the kinetics more fitted by a pseudo-second order indicated that the adsorption might also occur in chemical sorption. As isotherm results also supported the study of mechanism adsorption. The adsorption isotherm was studied based on the interaction of bulky adsorbate and the quantity of adsorbed dye. Based on isotherm results, Langmuir indicated that the adsorption sites have the same energy level and adsorption occurs at specific homogeneous sites on the surface. The homogenous surface of adsorbate also supported the even allocation on the surface [39]. The schematic of the adsorption mechanism of target pollutants by prepared LDH-chitosan adsorbent is shown in Figure 6.

4. Conclusion

The Zn/Al, Mg/Al, Zn/Al-Chitosan, and Mg/Al-Chitosan exhibited direct dye selective adsorption and all adsorbents are more selective for direct yellow-12 in an aqueous solution. The results data showed that Zn/Al, Mg/Al, Zn/Al-Chitosan, and Mg/Al-Chitosan have adsorption capacities 68.02, 135.13, 294.11, and 322.58 mg/g, respectively. According to these results, direct yellow-12 is more adsorbed by anion exchange for Mg/Al-chitosan and Zn/Al-chitosan than pristine ones. The adsorption mechanism also showed that the adsorption study suggested that the interaction of adsorbate and adsorbent was chemisorption.

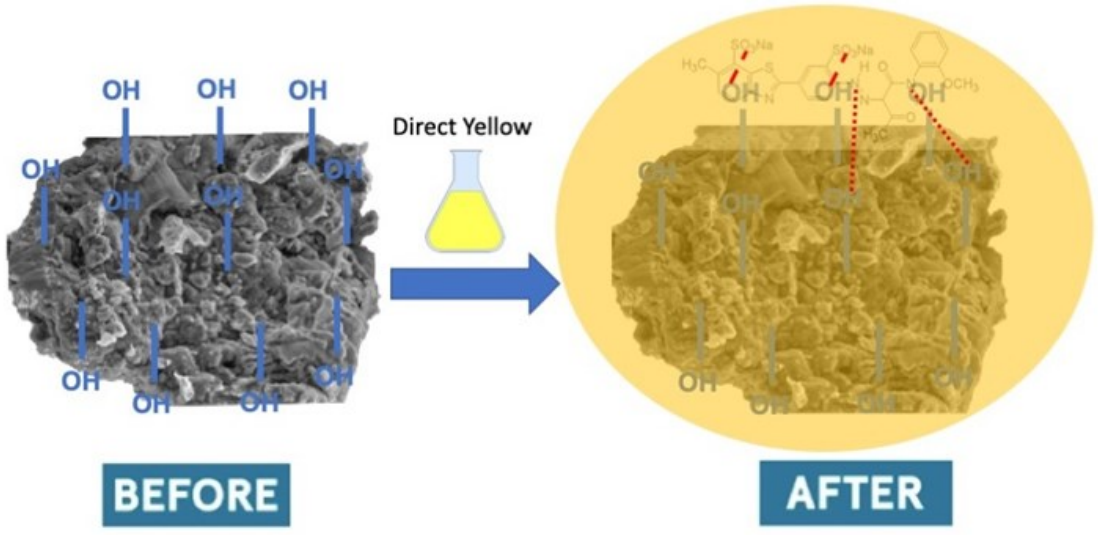

Figure 6. The adsorption mechanism of direct yellow using LDH-chitosan.

Table 5. Comparison results of adsorption by several adsorbents.

Adsorbents	q_{max} (mg/g)	Refs.
Corncob	65.03	[33]
Orange peel	75.7	[34]
ZnS:Mn-NPa-AC	90.0	[35]
Apatitic Tricalcium Phosphate	67.0	[36]
Zeolite	83.3	[37]
Zn/Al-chitosan	294.11	This study
Mg/Al-chitosan	322.58	This study

Acknowledgement

The authors had a special thanks to the Research Centre of Inorganic Materials and Complexes FMIPA Universitas Sriwijaya for support of instrumental, analysis, and valuable comments on this research.

CRediT Author Statement

Author Contributions: N. R. Palapa: Investigation, Resources, Data Curation, Writing, Review and Editing; N. Yuliasari: Methodology, Formal Analysis, Data Curation, Project Administration; P.M.S.N. Siregar: Validation, Writing, Review and Editing, Data Curation; A. Wijaya, A. Amri and Nur Ahmad: Investigation, Resource, Review and Editing, Validation. A. Lesbani: Conceptualization, Methodology, Investigation, Resources, Data Curation, Writing, Review and Editing, Supervision. All authors have read and agreed to the published version of the manuscript.

References

[1] Khataee, A., Leila, A., Hassani, A., Karaca, S. (2013). Response surface analysis of removal of a textile dye by a Turkish coal powder. *Advances in Environmental Research*, 2(4), 291–308. DOI: 10.12989/aer.2013.2.4.291.

[2] Yadav, B.S., Dasgupta, S. (2022). Effect of time , pH , and temperature on kinetics for adsorption of methyl orange dye into the modified nitrate intercalated MgAl LDH adsorbent. *Inorganic Chemistry Communications*, 137, 109203. DOI: 10.1016/j.inoche.2022.109203.

[3] Karimi-Maleh, H., Shafieizadeh, M., Taher, M.A., Opoku, F., Kiarii, E.M., Govender, P.P., Ranjbari, S., Rezapour, M., Orooji, Y. (2020). The role of magnetite/graphene oxide nanocomposite as a high-efficiency adsorbent for removal of phenazopyridine residues from water samples, an experimental/theoretical investigation. *Journal of Molecular Liquids*, 298, 112040. DOI: 10.1016/j.molliq.2019.112040.

[4] Ismail, A.M., Menazea, A.A. (2021). Selective adsorption of cationic azo dyes onto zeolite nanorod-based membranes prepared via laser ablation. *Journal of Materials Science: Materials in Electronics*, 32(14), 19352–19367. DOI: 10.1007/s10854-021-06453-w.

[5] Gong, X., Lu, H., Li, K., Li, W. (2022). Effective adsorption of crystal violet dye on sugarcane bagasse – bentonite / sodium alginate composite aerogel : Characterisation, experiments, and advanced modelling. *Separation and Purification Technology*, 286, 120478. DOI: 10.1016/j.seppur.2022.120478.

[6] Wilfried, J., Kanhounnon, W.G., Kpotin, G., Atohoun, G.S., Lain, J., Foucaud, Y., Badawi, M. (2021). Molecular insights on the adsorption of some pharmaceutical residues from wastewater on kaolinite surfaces. *Chemical Engineering Journal*, 407, 127176. DOI: 10.1016/j.cej.2020.127176.

[7] Palapa, N.R., Taher, T., Normah, N., Lesbani, A. (2022). NiAl Layered Double Hydroxide / Rice Husk Composite for the Efficient Removal of Malachite Green. *Indonesian Journal of Chemistry*, 22(1), 142–156. DOI: 10.22146/ijc.68021.

[8] Dou, D., Wei, D., Guan, X., Liang, Z., Lan, L., Lan, X. (2022). Adsorption of copper (II) and cadmium (II) ions by in situ doped nano-calcium carbonate high-intensity chitin hydrogels. *Journal of Hazardous Materials*, 423, 127137. DOI: 10.1016/j.jhazmat.2021.127137.

[9] Mohammed, N., Lian, H., Shahidul, M., Strong, M., Shi, Z., Berry, R.M., Yu, H., Chiu, K. (2021). Selective adsorption and separation of organic dyes using functionalized cellulose nanocrystals. *Chemical Engineering Journal*, 417, 129237. DOI: 10.1016/j.cej.2021.129237.

[10] Teli, M.D., Sheikh, J. (2012). Extraction of chitosan from shrimp shells waste and application in antibacterial finishing of bamboo rayon. *International Journal of Biological Macromolecules*, 50(5), 1195–1200. DOI: 10.1016/j.ijbiomac.2012.04.003.

[11] Gürsesa, A., Hassani, A., M.Kıranşan, M., Açışlı, O., Karaca, S. (2014). Removal of methylene blue from aqueous solution using by untreated lignite as potential low-cost adsorbent : Kinetic , thermodynamic and equilibrium approach. *Journal of Water Process Engineering*, 2, 10–21. DOI: 10.1016/j.jwpe.2014.03.002.

[12] Liu, D., Gu, W., Zhou, L., Wang, L., Zhang, J., Liu, Y. (2022). Recent advances in MOF-derived carbon-based nanomaterials for environmental applications in adsorption and catalytic degradation. *Chemical Engineering Journal*, 427, 131503. DOI: 10.1016/j.cej.2021.131503.

[13] Feng, X., Long, R., Wang, L., Liu, C., Bai, Z., Liu, X. (2022). A review on heavy metal ions adsorption from water by layered double hydroxide and its composites. *Separation and Purification Technology*, 284, 120099. DOI: 10.1016/j.seppur.2021.120099.

[14] Sajid, M., Muhammad, S., Jillani, S., Baig, N., Alhooshani, K. (2022). Layered double hydroxide-modified membranes for water treatment : Recent advances and prospects. *Chemosphere*, 287, 132140. DOI: 10.1016/j.chemosphere.2021.132140.

[15] Karim, A.V., Hassani, A., Eghbali, P., Nidheesh, P.V. (2022). Nanostructured modified layered double hydroxides (LDHs) - based catalysts : A review on synthesis , characterization , and applications in water remediation by advanced oxidation processes. *Current Opinion in Solid State & Materials Science*, 26(1), 100965. DOI: 10.1016/j.cossms.2021.100965.

[16] Mohadi, R., Palapa, N.R., Lesbani, A. (2021). Preparation of Ca/Al-Layered Double Hydroxides/Biochar Composite with High Adsorption Capacity and Selectivity toward Cationic Dyes in Aqueous. *Bulletin of Chemical Reaction Engineering & Catalysis*, 16(2), 244–252. DOI: 10.9767/bcrec.16.2.10211.244-252.

[17] Palapa, N.R., Taher, T., Mohadi, R., Rachmat, A., Mardiyanto, M., Miksusanti, M., Lesbani, A. (2021). NiAl-layered double hydroxide intercalated with Keggin polyoxometalate as adsorbent of malachite green : kinetic and equilibrium studies. *Chemical Engineering Communications*, 209(5), 684–695. DOI: 10.1080/00986445.2021.1895773.

[18] Zhang, J., Lu, W., Zhan, S., Qiu, J., Wang, X., Wu, Z., Li, H., Qiu, Z., Peng, H. (2021). Adsorption and mechanistic study for humic acid removal by magnetic biochar derived from forestry wastes functionalized with Mg / Al-LDH. *Separation and Purification Technology*, 276, 119296. DOI: 10.1016/j.seppur.2021.119296.

[19] Jung, K., Yong, S., Choi, J., Hwang, M. (2021). Synthesis of Mg – Al layered double hydroxides-functionalized hydrochar composite via an in situ one-pot hydrothermal method for arsenate and phosphate removal : Structural characterization and adsorption performance. *Chemical Engineering Journal*, 420, 129775. DOI: 10.1016/j.cej.2021.129775.

[20] Wijaya, A., Siregar, P.M.S.B.N., Priambodo, A., Palapa, N.R., Taher, T., Lesbani, A. (2021). Innovative Modified of Cu-Al/C (C = Biochar, Graphite) Composites for Removal of Procion Red from Aqueous Solution. *Science & Technology Indonesia*, 6(4), 228–234. DOI: 10.26554/sti.2021.6.4.228-234.

[21] Madihi-bidgoli, S., Asadnezhad, S., Yaghoot-nezhad, A., Hassani, A. (2021). Azurobine degradation using Fe_2O_3@multi-walled carbon nanotube activated peroxymonosulfate (PMS) under UVA-LED irradiation : performance, mechanism and environmental application. *Journal of Environmental Chemical Engineering*, 9(6), 106660. DOI: 10.1016/j.jece.2021.106660.

[22] Lü, Z., Hu, F., Li, H., Zhang, X., Yu, S., Liu, M., Gao, C. (2019). Composite nanofiltration membrane with asymmetric selective separation layer for enhanced separation efficiency to anionic dye aqueous solution. *Journal of Hazardous Materials*, 19, 436–443. DOI: 10.1016/j.jhazmat.2019.01.086.

[23] Hassani, A., Faraji, M., Eghbali, P. (2020). Chemistry Facile fabrication of mpg-C_3N_4/Ag / ZnO nanowires / Zn photocatalyst plates for photodegradation of dye pollutant. *Journal of Photochemistry & Photobiology, A: Chemistry*, 400, 112665. DOI: 10.1016/j.jphotochem.2020.112665.

[24] Kameda, T., Horikoshi, K., Kikuchi, H., Kitagawa, F. (2021). Nano-Structures & Nano-Objects Kinetic and equilibrium analyses of lactate adsorption by Cu-Al and Mg-Al layered double hydroxides (Cu-Al LDH and Mg-Al LDH) and Cu-Al and Mg-Al layered double oxides (Cu-Al LDO and Mg-Al LDO). *Nano-Structures & Nano-Objects*, 25, 100656. DOI: 10.1016/j.nanoso.2020.100656.

[25] Tanabe, E.H., Missau, J., Assumpç, D. (2021). Highly efficient adsorbent for removal of Crystal Violet Dye from Aqueous Solution by CaAl / LDH supported on Biochar. *Applied Clay Science*, 214, 106297. DOI: 10.1016/j.clay.2021.106297.

[26] Amin, M.T., Alazba, A.A., Shafiq, M. (2020). LDH of NiZnFe and its composites with carbon nanotubes and data-palm biochar with efficient adsorption capacity for RB5 dye from aqueous solutions: Isotherm, kinetic, and thermodynamics studies. *Current Applied Physics*. 40, 90-100. DOI: 10.1016/j.cap.2020.07.005.

[27] Grover, A., Mohiuddin, I., Kumar, A., Singh, J., Vikrant, K., Kim, K., Brown, R.J.C. (2022). Magnesium/aluminum layered double hydroxides intercalated with starch for effective adsorptive removal of anionic dyes. *Journal of Hazardous Materials*, 424, 127454. DOI: 10.1016/j.jhazmat.2021.127454.

[28] Eddarai, E.M., Mouzahim, M. El, Boussen, R., Bellaouchou, A., Guenbour, A., Zarrouk, A. (2022). International Journal of Biological Macromolecules Chitosan-kaolinite clay composite as durable coating material for slow release NPK fertilizer. *International Journal of Biological Macromolecules*, 195, 424–432. DOI: 10.1016/j.ijbiomac.2021.12.055.

[29] Elanchezhiyan, S.S.D., Meenakshi, S. (2017). Synthesis and characterization of chitosan/Mg-Al layered double hydroxide composites for the removal of oil particles from oil in water emulsion. *International Journal of Biological Macromolecules*, 104, 1586-1595. DOI: 10.1016/j.ijbiomac.2017.01.095.

[30] Lyu, F., Yu, H., Hou, T., Yan, L., Zhang, X., Du, B. (2019). Efficient and fast removal of Pb 2+ and Cd 2+ from an aqueous solution using a chitosan/Mg-Al-layered double hydroxide nanocomposite. *Journal of Colloid and Interface Science*, 539, 184–193. DOI: 10.1016/j.jcis.2018.12.049.

[31] Li, S., Xu, H., Wang, L., Ji, L., Li, X., Qu, Z., Yan, N. (2021). Dual-functional Sites for Selective Adsorption of Mercury and Arsenic ions in $[SnS_4]_4$-/MgFe-LDH from Wastewater. *Journal of Hazardous Materials*, 403, 123940. DOI: 10.1016/j.jhazmat.2020.123940.

[32] Tuzen, M., Sarı, A., Saleh, T.A. (2018). Response surface optimization, kinetic and thermodynamic studies for effective removal of rhodamine B by magnetic AC/CeO2 nanocomposite. *Journal of Environmental Management*, 206, 170–177. DOI: 10.1016/j.jenvman.2017.10.016.

[33] Berber-Villamar, N.K., Netzahuatl-Muñoz, A.R., Morales-Barrera, L., Chávez-Camarillo, G.M., Flores-Ortiz, C.M., Cristiani-Urbina, E. (2018). Corncob as an effective, eco-friendly, and economic biosorbent for removing the azo dye Direct Yellow 27 from aqueous solutions. *PLoS One*, 13(4), 1–30. DOI: 10.1371/journal.pone.0196428.

[34] Khaled, A., Nemr, A. El, El-sikaily, A., Abdelwahab, O. (2009). Treatment of artificial textile dye effluent containing Direct Yellow 12 by orange peel carbon. *Desalination*, 238(1–3), 210–232. DOI: 10.1016/j.desal.2008.02.014.

[35] Hajati, S., Ghaedi, M., Karimi, F., Barazesh, B. (2013). Journal of Industrial and Engineering Chemistry Competitive adsorption of Direct Yellow 12 and Reactive Orange 12 on ZnS : Mn nanoparticles loaded on activated carbon as novel adsorbent. *Journal of Industrial and Engineering Chemistry*, 20(2), 564-571. DOI: 10.1016/j.jiec.2013.05.015.

[36] Boujaady, H.E., Mourabet, M., Taitai, A. (2013). Adsorption / desorption of Direct Yellow 28 on apatitic phosphate: Mechanism, kinetic and thermodynamic studies. *Journal of the Association of Arab Universities for Basic and Applied Sciences*, 16, 64-73. DOI: 10.1016/j.jaubas.2013.09.001

[37] Alabbad, E.A. (2021). Efficacy assessment of natural zeolite containing wastewater on the adsorption behaviour of Direct Yellow 50 from; equilibrium, kinetics and thermodynamic studies. *Arabian Journal of Chemistry*, 14(4), 103041. DOI: 10.1016/j.arabjc.2021.103041.

[38] Li, A., Zhang, Y., Ge, W., Zhang, Y., Liu, L., Qiu, G. (2022). Bioresource Technology Removal of heavy metals from wastewaters with biochar pyrolyzed from MgAl-layered double hydroxide-coated rice husk : Mechanism and application. *Bioresource Technology*, 347, 126425. DOI: 10.1016/j.biortech.2021.126425.

[39] Hossain, A., Mondol, M.H., Jhung, S.H. (2022). Chemosphere Functionalized metal-organic framework-derived carbon : Effective adsorbent to eliminate methylene blue, a small cationic dye from water. *Chemosphere*, 303, 134890. DOI: 10.1016/j.chemosphere.2022.134890.